A Lattice-Free Model Of Translocation-Induced Outgrowth In Fungal Mycelia

Iestyn Carver & Graeme P. Boswell *

Abstract— **Fungal mycelia occupy a central role in nutrient cycling and are widely used in biological control and remediation. In these settings, fungi form complex networks that develop in heterogeneous environments by uptaking nutrients from regions of local excess and transporting them to regions of local scarcity. In this work a novel mathematical model of mycelial growth is described that explicitly incorporates the irregular branched and interconnected nature of the mycelium and simulates the flow of internally-located material. The model is applied to a simple experimental configuration, representing mycelial growth from an isolated nutrient supply, and it is shown that a basic measurement of the developing network directly relates to the transportation mechanisms used by mycelial fungi.**

Keywords: anastomosis, fractal dimension, branching, mycelium, translocation.

1 Introduction

Mycelial fungi comprise a highly-branched and interconnected network of tubes, termed *hyphae*, that, despite their microscopic scale, are capable of extending over vast distances [1] and occupy an essential role in the cycling of various nutrients [2]. Moreover, certain fungal species form symbiotic connections with plant root systems and so allow the transfer of nutrients over far wider spatial scales than would be possible in their absence [3]. In addition to their ecological roles, recent work has focussed on the biotechnological applications of fungi, such as in biocontrol and bioremediation [4].

In all of the above contexts, mycelia develop over time by acquiring and *translocating* a range of nutrients, such as carbon, nitrogen and trace elements, through the network. This material is used to further extend the network structure, allowing the exploitation and colonization of distant nutrient resources [5]. Soils are the natural growth environment for many of these mycelia but because of the complex heterogeneities involved there are obvious difficulties in experimental investigations of their growth and function in such settings. Instead many experimental investigations have been conducted on mycelia grown on Petri dishes using either homogeneous conditions or carefully controlled nutritional heterogeneities [6]. However, because of the microscopic scale of hyphae in the fungal network, there are also inherent difficulties in the understanding and interpretation of results obtained in even these settings. Mathematical modelling thus provides a powerful complimentary technique to augment experimental investigation and has been consistently used to aid in the understanding of mycelial growth and function (see, for example, the extensive reviews in [7, 8]).

Many mathematical models treat the mycelium as a continuous structure [9, 10, 11, 12, 13]. While that approach is highly successful for modelling dense networks, it is not suited for modelling the sparse networks that arise under low nutrient conditions since the underlying network formation is neglected. However, there have been a number of discrete models that do account for the branched and interconnected characteristics of the mycelium and essentially these models can be classified as being either *lattice-based* or *lattice-free*.

A lattice-based model is essentially a cellular automata where the modelled network is confined to a regular grid [14, 15, 16]. The regular geometry of the network allows the incorporation of branching and *anastomosis* (the fusion of the network into itself). Moreover, as in [15, 16], the uptake of nutrients by the network can be modelled along with their resultant translocation. However, since growth is confined to a lattice, the regular geometry of the resultant network does not best represent the more irregular characteristics of mycelial fungi.

A popular alternative approach to simulating mycelial networks involves a lattice-free approach [17, 18, 19], which places no restriction on the position of the network. The modelled network comprises connected line segments and while such models are capable of generating structures that are highly reminiscent of mycelial fungi, they have typically neglected many processes crucial to their growth habit. For example, anastomosis has previously been ignored, often because of the overwhelming computational difficulties (but see [20] for an angiogenesis model that includes anastomosis). For similar reasons, translocation has also been neglected. Those two processes, in particular, are essential for the growth and function of

*Division of Mathematics and Statistics, Faculty of Advanced Technology, University of Glamorgan, Pontypridd, CF37 1DL, U.K. Email: gpboswel@glam.ac.uk.

mycelial fungi expanding in heterogeneous conditions and hence must be considered in any model capable of quantitative predictions.

In this work a lattice-free approach incorporating anastomosis has been used to model a mycelium growing on a planar surface and, for the first time in a lattice-free model, translocation within the network was also included. To achieve this, the entire network was recorded in a manner that allowed a systematic approach to locating all its connections. Section 2 contains a description of the technique used to store the network and the rules that governed its development. In Section 3 the model is applied to investigate a standard experimental system representing the outgrowth of a mycelium from a nutrient source into a nutrient-free environment and the implications of the modelling approach are discussed in Section 4.

2 Modelling

The mycelial network was modelled as a collection of connected line segments of a fixed length h positioned on a plane so that a single hypha was represented by a series of such line segments. For simplicity and as a necessary first step, it was assumed that a single generic substrate was responsible for hyphal growth and that the substrate concentration was uniform within each line segment, but allowed to be different between connected line segments. (In previous models, this substrate was often regarded as carbon, see, for example, [15].) Each line segment was represented by a four dimensional structure $v = (x, y, \theta, E)$ where x and y were the Cartesian coordinate position of the start of the line segment, $\theta \in (-\pi, \pi]$ denoted the angle of the line segment measured with respect to the positive x-axis and E denoted the amount of substrate contained in the line segment.

The entire network was recorded in a dynamic two dimensional array denoted by M whose entries were the structures v defined above and where each row corresponded to a hyphae. The initial configuration of the network consisted of a number N_0 of line segments each starting from the origin and radiating outwards in randomly chosen directions containing a specified amount E_0 of substrate. This starting configuration was thus represented by an array of N_0 rows and a single column.

Time was modelled to advance in discrete steps and at the end of each time step the network could expand due to the creation of new hyphae (branching), the lengthening of existing hyphae, the fusion of hyphae (anastomosis) and the movement of substrate within the network (translocation). The columns of the array M corresponded to the time that a line segment was created and so at the end of every time step a new column was amended to M and the substrate levels in all line segments throughout the array were updated. To quantify the resultant network, its approximate box counting fractal dimension was calculated at the end of each time step. Each of these processes are described in detail below.

2.1 Branching

Experimental studies have shown that branching in mycelial fungi is caused by a combination of turgor pressure and a local accumulation of tip vesicles [21, 22], which arise through the acquisition of suitable nutrients. Consequently for the modelling it was assumed that the branching rate in a line segment was proportional to the amount of substrate contained within that segment. (A similar approach has been successfully applied previously [12, 15].) Branching was assumed dichotomous, which is known to occur in certain fungi including *Allomyces macrogynus*, *Galactomyces geotrichum* [23] and *Aspergillus niger* [24]. Therefore a line segment at the periphery of the network underwent branching with probability bE where b was a non-negative constant and E denoted the substrate contained within that line segment. To simulate that process, a uniformly distributed random number was selected in the interval $[0, 1]$ and if that number was less than bE then a branching event would occur. (If bE exceeded unity then branching definitely occurred.) In such an event two new line segments were created where each originated from the end of the existing line segment. The direction of these new line segments were given by $\theta \pm \xi$ where θ was the angle of the existing line segment and ξ was a random variable selected from $N(0, \sigma^2)$, a normal distribution of mean 0 and standard deviation σ (Fig 1 (a)). The substrate in each line segment was then calculated which, for improved exposition, is described below in Section 2.5.

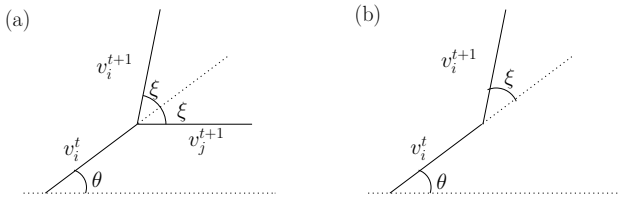

Figure 1: (a) The line segment v_i^t at angle θ to the horizontal x-axis undergoes branching generating two new line segments with angles to the horizontal being $\theta \pm \xi$, where $\xi \in N(0, \sigma^2)$. One of the new line segments (v_i^{t+1}) is assigned to the existing line segment while the other (v_j^{t+1}) is regarded as a new hyphae. (b) A new line segment v_i^{t+1} extends from an existing line segment v_i^t at an angle $\xi \in N(0, \sigma^2)$.

After a branching event, one of the new line segments was assigned to the existing hyphae while the other new line segment was regarded as a new hyphae and was represented by a new row in the array M storing the entire network. This new row started with a sufficient number

of null entries so that the two new line segments appeared in the same column. Additionally, to facilitate the modelling of substrate movement, the location of the three connected line segments in the matrix M were stored in another array B which held the location of all branching points in the network and the corresponding line segments.

2.2 Hyphal extension

In addition to their role in branching, tip vesicles are primarily responsible for the extension of hyphae [22, 23]. Indeed, in the absence of internal nutrients, there is no supply of vesicles to the extending ends of hyphae and consequently no growth. The straight line hyphal growth habit is thus a consequence of the supply of tip vesicles to the extending ends of hyphae and where variations in the supply of the vesicles result in minor changes of the growth direction [25].

The model incorporated hyphal extension by examining those line segments at the periphery of the network that did not undergo branching. Provided there was sufficient energy in each segment, modelled by the substrate level exceeding an amount c, the hyphae extended by generating a new line segment starting from the end of the existing segment and whose direction was $\theta + \xi$ where, as above, θ denoted the direction of the existing line segment with respect to the positive x-axis and ξ was a random variable taken from $N(0, \sigma^2)$ (Fig 1 (b)), where σ denoted the standard deviation of the turning angle. The new line segment was amended to the end of the corresponding row of the network array M. The substrate in the new line segment was calculated (described below).

It was assumed that the hyphae did not have sufficient energy to extend when the substrate level was less than c. In such cases, no new line segments were created and instead a null structure was placed in the appropriate position in the network array M.

The above modelling approach implies that hyphae extend in a pulsed manner (that is, hyphae move or do-not-move) and, on average, in a straight line, which has long been observed in certain mycelial fungi [26]. Moreover, experimental evidence shows that the variation in hyphal extension is random [27], a property encapsulated in the model construction.

2.3 Growth costs

As a mycelium grows, internally-located nutrients are used to construct new wall material [23] and thus the growing ends of hyphae represent energy sinks. To model this process it was assumed that the formation of a new line segment from an existing line segment (either through branching or hyphal extension) would result in a reduction of the substrate level in the originating line segment by an amount c representing the energy cost of forming a length h of hyphae. Since hyphal extension was possible only when the substrate level exceeded the amount c, the substrate levels in a line segment remained non-negative.

2.4 Anastomosis

If any of the new line segments created through branching or hyphal extension intersected an existing line segment then they were assumed to anastomose, that is, fuse with each other. To this end, all new line segments were systematically checked to see if they intersected any of the previous line segments and if an intersection occurred the new line segment was revised so that it fused with the existing network at the first point of intersection. (Multiple intersections were a possibility, especially in dense networks.) This was accounted for by setting the next entry in the corresponding row of M with a carefully selected structure $\hat{v} = (\hat{x}, \hat{y}, \hat{\theta}, \hat{E})$, where $\hat{x}$ and $\hat{y}$ denoted the Cartesian coordinate position of the first intersection and $\hat{\theta}$ took a null value indicating the structure $\hat{v}$ did not represent a line segment. To facilitate substrate movement within the network, the location of the line segments involved in the anastomoses were recorded in another array denoted by A.

2.5 Substrate concentrations

The model was applied to simulate outgrowth experiments where mycelia expand from an isolated nutrient source into a nutrient-free domain [28]. In such a situation, mycelial growth is only possible because the nutrients acquired at the source are translocated through the network.

In the model it was assumed that the substrate source at the origin was continually replenished and acquired by the mycelium, either through active transport or diffusion across the hyphal wall [11] and, consistent with experimental data, was in excess of local needs [29]. Thus fixed boundary conditions were used to represent the uptake of the substrate by the mycelium at the origin by setting the original N_0 line segments to contain a substrate concentration of E_0.

Since diffusion plays a significant role in the translocation of several key nutrients, including carbon, throughout the hyphal network [29, 30], substrate movement was modelled accordingly. Specifically, the change of substrate in a line segment k over the time step was given by

$$\Delta E_k = \sum_{\substack{\text{connected} \\ \text{segments } j}} D \, \frac{E_j - E_k}{h} \qquad (1)$$

where the diffusion coefficient D was sufficiently small with respect to h to ensure numerical stability. (In all our simulations the values of h and D were chosen such

Table 1: A description of the parameters and their values used in the simulations.

Parameter	*Description*	*Value (unless otherwise stated)*
h	Length of line segment	1
N_0	Initial number of hyphae/line segments	15
E_0	Substrate at origin	10^0 – 10^5
b	Branching rate at tip	0.5
σ	Standard deviation of hyphal tip movement	0.2
c	Cost of growth of unit length	0.02
D	Diffusion coefficient for substrate	0.01 – 0.4

that numerical stability was assured.) It was straightforward to account for translocation between connected line segments along what represented the same hyphae since they corresponded to adjacent line segments on the same row of the array M. The inclusion of any additional connected line segments that occurred through branching or anastomosis was achieved by systematically accounting for the connections that were recorded in the arrays B and A that identified the location of branches and anastomoses in the network respectively.

While this modelling approach does not include metabolically-driven translocation mechanisms that are known to occur in certain mycelial fungi [29], it does however represent an important and necessary first step in modelling substrate movement through an irregular and continually changing network.

2.6 Fractal dimension

To quantify the modelled mycelial network (and to allow comparison with experimental data, e.g. [31, 32]), the box counting fractal dimension of the network was approximated at the end of each time step. This process was implemented by covering the simulated network by a series of square meshes of different sizes and counting the number of squares that contained a line segment for each mesh. The counting process was conducted by locating all the intersections of each line segment in the network with the mesh using the same algorithmic approach adopted in the location of all the anastomoses in the network. Thus the occupied squares in each mesh were obtained and the negative gradient of the regression line of the logarithm of the number of occupied squares against the logarithm of the mesh size gave the fractal dimension of the simulated network.

3 Results

3.1 Effect of substrate supply on outgrowth

The model was simulated for values of E_0, corresponding to different amounts of substrate available at the origin, ranging between 10^0 and 10^5, where 20 runs were performed for each value of E_0. The other parameter values are specified in Table 1 with the diffusion coefficient taken as $D = 0.4$.

The initial development of the network was largely independent of E_0 since the amount of substrate transported to the expanding hyphal tips was sufficient to promote growth and branching (Fig. 2). However, as the network expanded, the substrate had to diffuse over longer distances and so there was an increasing dependence of E_0 on further network growth. Thus, for small values of E_0, there was minimal branching distant from the origin resulting a sparse mycelial network (Fig. 2(a)). However, for progressively larger values of E_0, the effective diffusion range increased because of the increased substrate gradient (see equation (1)), which resulted in increased branching and hence an increase in the network density (Fig. 2(b),(c),(d)).

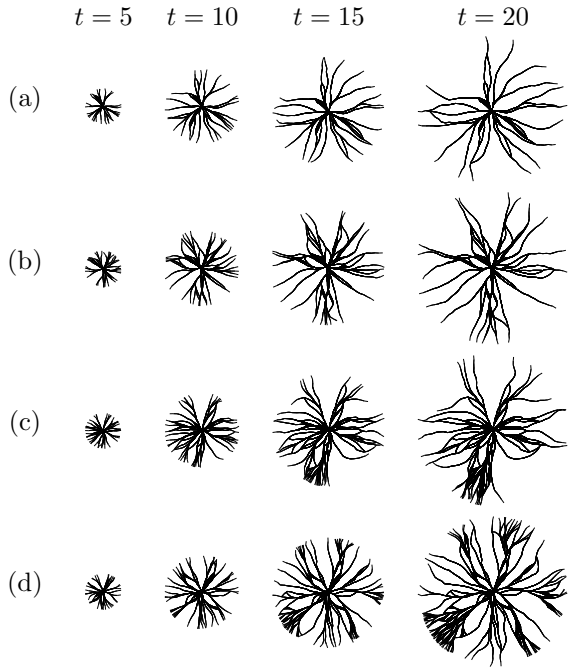

Figure 2: Simulated networks at times $t = 5, 10, 15$ and 20 using the parameter values in Table 1 with $D = 0.4$ and (a) $E_0 = 10^1$, (b) $E_0 = 10^2$, (c) $E_0 = 10^3$ and (d) $E_0 = 10^4$.

Since the networks comprised connected line segments of length at most h, the box sizes used to determine the

fractal dimension ranged between $h/100$ up to h. (This choice of box sizes ensured that a single unconnected line segment had a fractal dimension of unity, whereas using larger box sizes would lead to an unrealistic box counting dimension of less than unity.) The fractal property existed across this range of box sizes as evidenced by a linear relationship between the logarithms of the box size and the number of boxes required to cover the network (Fig. 3).

The fractal dimension of the simulated networks changed over time depending on the substrate available at the origin (Fig. 4). Except for the smallest value of E_0, the fractal dimension initially increased but then declined because the space behind the network periphery was unfilled due to a lack of branching. For small values of E_0, there was a low branching frequency resulting in a continual decline in the fractal dimension. However, for progressively larger values of E_0, the decline in the fractal dimension was less and when $E_0 \geq 10^4$ the fractal dimension later increased because the increased branching frequency brought about by an abundance of substrate in the network resulted in a more complete coverage of space behind the network periphery (Fig. 2(d)). In most cases, different initial substrate levels resulted in networks having significantly different fractal dimensions by the 20^{th} time step (1-way ANOVA, Table 2).

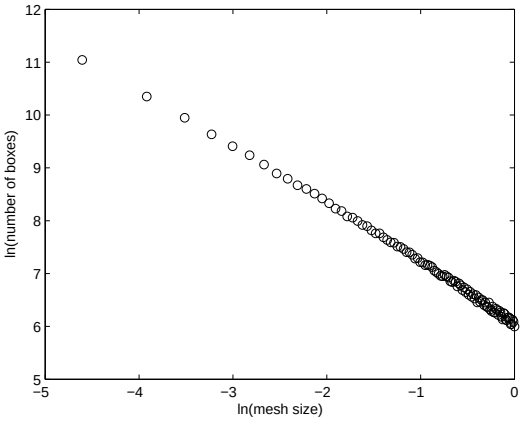

Figure 3: The natural logarithm of the number of boxes used to cover a network at time $t = 20$ with initial data $E_0 = 10^3$, $D = 0.4$ and other parameters given in Table 1 was plotted against the natural logarithm of the mesh size for 101 uniformly distributed meshes between $h/100$ and h. The linear relationship between the data ensured the fractal approximation was valid across the entire range of mesh sizes considered.

3.2 Effect of translocation rates on outgrowth

The model was simulated to represent fungi with different translocation rates cultured in the same environment by varying only the substrate diffusion rate D between 0.01 and 0.4. Twenty simulations were performed over 20 time iterations for each value of D where $E_0 = 10^4$ and with other parameters given in Table 1. The box counting dimension of the resultant networks were calculated at each time iteration for each value of D (Fig. 5). In all but one case ($D = 0.4$) it was observed that the mean box counting dimension of the networks decayed over time and the greatest decay rates corresponded to the smallest diffusion rates. For the remaining case $D = 0.4$ the box counting dimension increased over the time duration considered, but this increase was only transient as separate simulations performed over a longer time period showed the box counting dimension eventually decayed toward unity as the network expanded further in the same qualitative manner as the cases $D < 0.4$ (data not shown).

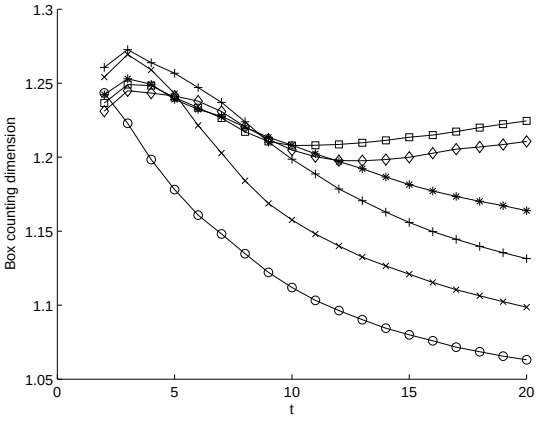

Figure 4: The mean fractal dimensions for 20 simulations with initial data $E_0 = 10^0$ ($\circ$), $E_0 = 10^1$ ($\times$), $E_0 = 10^2$ ($+$), $E_0 = 10^3$ ($*$), $E_0 = 10^4$ ($\square$) and $E_0 = 10^5$ ($\diamond$). Other parameters are specified in Table 1 with $D = 0.4$. For improved exposition, error bars are not shown but Table 2 shows that there were significant differences at time $t = 20$ between most of the graphs.

4 Discussion

The vector-based approach adopted in this work, coupled with the inclusion of anastomosis, has resulted in the most visually impressive modelled mycelial networks in the literature to date. By including translocation as a simple diffusive process, which has long been known to occur in many mycelial fungi, there is also a strong mechanistic underpinning to the model which is essential if the model is to be used as a predictive tool.

Mycelial fungi grow from an isolated nutrient supply because of their ability to acquire and translocate materials from the nutrient source to the hyphal tips. In the model it was assumed that translocation occurred

Table 2: The fractal dimension of simulated networks at time $t = 20$ generated by different initial substrate levels are compared using a one-way ANOVA test. The p-values are shown for comparisons between different data sets and there were significant differences except in the two cases indicated.

E_0	10^0	10^1	10^2	10^3	10^4	10^5
10^0	–	$p < 0.001$	$p < 0.001$	$p < 0.001$	$p < 0.001$	$p < 0.001$
10^1	–	–	$p < 0.02$	$p < 0.001$	$p < 0.001$	$p < 0.001$
10^2	–	–	–	Not sig.	$p < 0.05$	$p < 0.05$
10^3	–	–	–	–	$p < 0.05$	$p < 0.05$
10^4	–	–	–	–	–	Not sig.

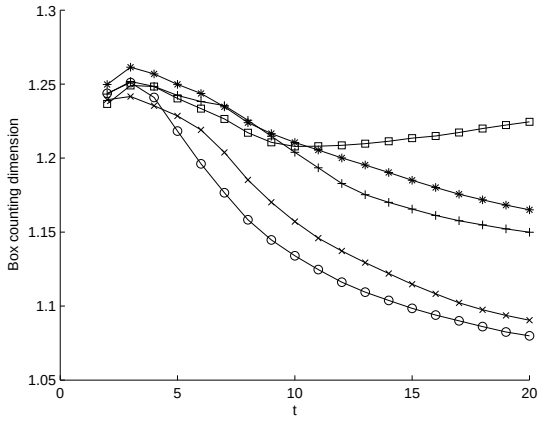

Figure 5: The model was simulated twenty times with $E_0 = 10^4$ for different values of D for twenty iterations and the mean box counting dimension is shown; $D = 0.01$ ($\circ$), $D = 0.1$ ($\times$), $D = 0.2$ ($+$), $D = 0.3$ ($*$) and $D = 0.4$ ($\square$). The other parameter values are stated in Table 1.

solely by diffusion acting between segments of hyphae within the mycelium. The amount of material translocated within the network increased with the gradient of substrate between hyphal segments, which itself occurred through either increased nutrient supply at the origin or an increase in the diffusion coefficient D. In both cases the density of the hyphae in the modelled networks, along with their fractal dimension, increased with translocation rates. However, because the translocation process was governed by diffusion, when the network reached a certain radius the amount of substrate diffusing from the nutrient source to the network periphery became negligible resulting in minimal further branching. In turn, all subsequent growth was mostly confined to the extension of hyphae and hence the fractal dimension of the mycelium eventually declined to unity since the periphery of the network mainly comprised unconnected line segments. The simulations thus predict that a quantitative measure of the diffusion-based translocation rate within a mycelium can be determined by observing the time taken for the fractal dimension of the mycelium to approach unity when forming under outgrowth conditions.

If translocation has more than just a diffusive component, (as is known to occur for certain nutrients in particular fungi, [29]), then the structure of the mycelium and its fractal dimension obtained under outgrowth conditions is likely to be very different. For example, a directed translocation component would ensure a more consistent branching rate, even long distances from the nutrient supply, which should manifest itself with the fractal dimension tending to an asymptotic value greater than unity.

The modelling has suggested that a simple qualitative measurement of a fungi's ability to translocate is given by examining the mycelia produced under outgrowth conditions and investigating how their fractal dimension change over time. Furthermore, such an experiment could also provide information on the translocation mechanisms themselves.

References

[1] M.L. Smith, J.N. Bruhn, J.B. Anderson, "The fungus *Armillaria bulbosa* is among the largest and oldest living organisms," *Nature* vol. 356, 1992, pp. 428–431.

[2] G.M. Gadd, "Fungal production of citric and oxalic acid: importance in metal speciation, physiology and biogeochemical processes," *Advances in Microbial Physiology* vol. 41, 1999, pp. 47–92.

[3] L. Boddy, "Saprotrophic cord-forming fungi: meeting the challenge of heterogeneous environments," *Mycologia* vol. 91, 1999, pp.13–32.

[4] J.M. Whipps, "Microbial interactions and biocontrol in the rhizosphere," *Journal of Experimental Botany* vol. 52, 2001, pp. 487–511.

[5] G.F. Morley, J.A. Sayer, S.C. Wilkinson, M.M. Gharieb, G.M. Gadd, "Fungal sequestration, solubilization and transformation of toxic metals," in *Fungi and Environmental Change* J.C. Frankland, N. Magan, G.M. Gadd (Eds.). Cambridge: Cambridge University Press, 1996, pp.235–256.

[6] H. Jacobs, G.P. Boswell, C.M. Scrimgeour, F.A. Davidson, G.M. Gadd, K. Ritz, "Translocation of glucose-derived carbon by *Rhizoctonia*

solani in nutritionally heterogeneous environments," *Mycological Research* vol. 108, 2004, pp. 453–461.

[7] J.I. Prosser, "Mathematical modelling of fungal growth," in *The Growing Fungus* N.A.R. Gow and G.M. Gadd (Eds.). London: Chapman and Hall, 1995, pp. 319–335.

[8] F.A. Davidson, "Mathematical modelling of mycelia: a question of scale," *Fungal Biology Reviews* vol. 21, 2007, pp. 30–41.

[9] L. Edelstein, "The propagation of fungal colonies: a model for tissue growth," *Journal of Theoretical Biology* vol. 98, 1982, pp. 679–701.

[10] F.A. Davidson, B.D. Sleeman, A.D.M. Rayner, J.W. Crawford, K. Ritz, "Large scale behaviour of fungal mycelia," *Mathematical and Computer Modelling* vol. 24, 1996, pp. 81–87.

[11] F.A. Davidson, "Modelling the qualitative response of fungal mycelia to heterogeneous environments," *Journal of Theoretical Biology* vol. 195, 1998, pp. 281–292.

[12] G.P. Boswell, H. Jacobs, F.A. Davidson, G.M. Gadd, K. Ritz, "Growth and function of fungal mycelia in heterogeneous environments," *Bulletin of Mathematical Biology* vol. 65, 2003, pp. 447–477.

[13] R.E. Falconer, J.L. Brown, N.A. White, J.W. Crawford, "Biomass recycling and the origin of phenotype in fungal mycelia," *Proceedings of the Royal Society B: Biological Sciences* vol. 272, 2006, pp. 1727–1734.

[14] G.B. Ermentrout, L. Edelstein-Keshet, "Cellular automata approaches to biological modelling," *Journal of Theoretical Biology* vol. 160, 1993, pp. 97–133.

[15] G.P. Boswell, H. Jacobs, K. Ritz, G.M. Gadd, F.A. Davidson, "The development of fungal networks in complex environments," *Bulletin of Mathematical Biology* vol. 69, 2007, pp. 605–634.

[16] G.P. Boswell, "Modelling mycelial networks in structured environments," *Mycological Research* vol. 112, 2008, pp. 1015–1025.

[17] D. Cohen, "Computer simulation of biological pattern generation processes," *Nature* vol. 216, 1967, pp. 246–248.

[18] A.D. Bell, "The simulation of branching patterns in modular organisms," *Philisophical Transactions of the Royal Society of London B, Biological Sciences* vol. 313, 1986, pp. 143–160.

[19] A. Meškauskas, M.D. Fricker, D. Moore, "Simulating colonial growth of fungi with the neighbour-sensing model of hyphal growth," *Mycological Research* vol. 108, 2004, pp. 1241–1256.

[20] M.J. Plank, B. Sleeman, "Lattice and non-lattice models for tumour angiogenesis," *Bulletin of Mathematical Biology* vol. 66, 2004, pp. 1785–1819.

[21] J. Webster, *Introduction to Fungi* (2^{nd} ed.). Cambridge: Cambridge University Press, 1980.

[22] N.A.R. Gow, G.M. Gadd (Eds.), *The Growing Fungus*. London: Chapman and Hall, 1995.

[23] J. Webster, R. Weber, *Introduction to Fungi* (3^{rd} ed.). Cambridge: Cambridge University Press, 2007.

[24] C.G. Reynaga-Peña, G. Gierz, S. Bartnicki-García, "Analysis of the role of the Spitzenkörper in fungal morphogenesis by computer simulation of apical branching in *Aspergillus niger*," *Proceedings of the National Academy of Sciences USA* vol. 94, 1997, pp. 9096-9101.

[25] M. Riquelme, C.G. Reynaga-Peña, G. Gierzb, S. Bartnicki-García, "What determines growth direction in fungal hyphae?," *Fungal Genetics and Biology* vol. 24, 1998, pp. 101–109.

[26] R. Lopez-Franco, S. Bartnicki-García, C.E. Bracker, "Pulsed growth of fungal hyphal tips," *Proceedings of the National Academy of Sciences USA* vol. 91, 1994, pp. 12228-12232.

[27] K. Sampson, R.R. Lew, I.B. Heath, "Time series analysis demonstrates the absence of pulsatile hyphal growth," *Microbiology* vol. 149, 2003, pp. 3111-3119.

[28] C. Persson, S. Olsson, H.-B. Jansson, "Growth of *Arthrobotrys superba* from a birch wood food base into soil determined by radioactive tracing," *FEMS Microbiology Ecology* vol. 31, 2000, pp. 47–51.

[29] S. Olsson, "Mycelial density profiles of fungi on heterogeneous media and their interpretation in terms of nutrient reallocation patterns," *Mycological Research* vol. 99, 1995, pp. 143–153.

[30] S. Olsson, D.H. Jennings, "Evidence for diffusion being the mechanism of translocation in the hyphae of three molds," *Experimental Mycology* vol. 15, 1991, pp. 302–309.

[31] K. Ritz, J.W. Crawford, "Quantification of the fractal nature of colonies of *Trichoderma viride*," *Mycological Research* vol. 94, 1990, pp. 1138–1141.

[32] L. Boddy, J.M. Wells, C. Culshaw, D.P. Donnelly, "Fractal analysis in studies of mycelium in soil," *Geoderma* vol. 88, 1999, pp. 301–328.